IEEE Open Journal of the
Industrial Electronics Society

Received 26 August 2021; revised 3 October 2021; accepted 14 October 2021. Date of publication 19 October 2021;
date of current version 4 November 2021. The review of this paper was arranged by Associate Editor Hiralal Murlidhar Suryawanshi.

Digital Object Identifier 10.1109/OJIES.2021.3121088

A Novel In-Situ Measurement Method of High-Frequency Winding Loss in Cored Inductors With Immunity Against Phase Discrepancy Error

NAVID RASEKH (Student Member, IEEE), JUN WANG (Member, IEEE), AND XIBO YUAN (Senior Member, IEEE)

Department of Electrical and Electronic Engineering, University of Bristol, Bristol BS8 1UB, U.K.

CORRESPONDING AUTHOR: XIBO YUAN (e-mail: xibo.yuan@bristol.ac.uk).

This work was supported in part by the U.K. Royal Academy of Engineering.

ABSTRACT Evaluating the high-frequency winding loss accurately is crucial for the design of modern high-frequency power converters. This paper proposes a novel experimental method to accurately measure the in-situ inductor winding loss, which separates out the winding loss from the core loss through the reactive voltage cancellation concept. The proposed in-situ measurement can account for the complete winding loss including impacts from non-ideal field distributions by testing the inductor with the core attached, e.g., the winding edge effect, bypass flux, fringing flux, and the non-linear dynamic behaviour of the core, which cannot be well modelled with the existing analytical or simulation methods. This method has immunity against the probe phase discrepancy error, since it is designed to measure a pair of voltage and current that are in phase. This approach can be considered as the first attempt of applying the reactive voltage cancellation concept in measuring winding loss, while this concept was originally brought up for core loss and applied for core loss measurement only. By performing a Triple Pulse Test (TPT) procedure, the winding losses under practical large signals with dc-bias and rectangular voltage can be evaluated with the proposed testing circuit. The proposed approach is compared and verified against the conventional methods relying on (1) small-signal impedance measurements and FFT analysis (2) in-situ measurement with the two winding method to exclude the core loss. The presented method provides a foundation for the accurate in-situ evaluation of winding loss covering all the large-signal and non-linear effects.

INDEX TERMS Winding loss, copper loss, AC resistance, phase shift error, phase discrepancy.

1. INTRODUCTION

Along with the advances of high-switching-frequency power converters, the winding loss of the magnetic components makes considerable impacts on the converter efficiency and temperature rise. Given passive components normally account for around 30%–50% of the total volume/weight of a typical power electronics system, how to accurately model/evaluate the high-frequency loss of magnetic components is critical for the precise design of the system. While the modelling of core loss has drawn numerous research efforts recently [1]–[4], the winding loss is commonly modelled by long-established analytical AC resistance models and Fourier analysis, e.g., [5]–[8] or finite-element (FE) simulations [9]–[12]. However, these approaches are typically limited by over-simplifying (e.g., 1-D and 2-D simulations or analytical models with assumptions for simplicity), which are briefly discussed as follows.

In general, the winding loss is analyzed with Fourier series as

$$P_{Winding} = R_{DC}.{I_{DC}}^2 + \sum_{n=1}^{\infty} {I_n}^2.R_{ACn} \tag{1}$$

where R_{DC} and I_{DC} are the DC resistance and DC current; R_{ACn} and I_n are the AC resistance and AC RMS current harmonics in each frequency. R_{DC} can be relatively easy to retrieve, such as measured by high precision milliohm meter or calculated from analytical equations [5], owing to its constant value at different operation conditions. However, R_{ACn} is the main challenge to find under various conditions. In general, R_{ACn} can be found analytically (e.g., through the Dowell or Ferreira equations [6-7]) or through FE simulations.

However, the analytical and simulation methods are limited by requiring accurate geometrical information of the windings considering the shape and the configuration (e.g., porosity factor, end winding, multilayers) [8], which is especially challenging for random-wound inductors and in-situ measurements. Therefore, analytical methods are normally applied for cases with only simple core shapes and simple winding arrangements. On top of that, the increasing high-frequency operation of magnetic components with wide-bandgap (SiC, GaN) converters will intensify the high-frequency effects such as skin, proximity, and fringing fields effect, which are very challenging to analytically model or simulate accurately [10]. Furthermore, the actual current I in equation (1) cannot be well predicted by the analytical models or simulations because of the non-linear permeability of the magnetic core in dynamic and dc-biased cases, which cannot be fully reflected by physical-based models [13]. Under the high-frequency rectangular excitation voltage, the inductance of the magnetic components is not constant and the current is not strictly triangular, which instead will show a curvy shape [3], [13]. However, the inductance and the permeability of the core is commonly considered constant in analytical models or simplified simulations. Although FE simulations can be built with increased complexity (e.g., 3-D FE models) to account for the complex high-frequency electromagnetic effects, they are less favoured in practice due to the disadvantage of the computation-heavy, time-consuming process [10]–[11] and the inevitable need of accurately replicating the geometrical structure of the components.

Owing to the above limitations of the analytical and simulation approaches, empirical measurement methods are still widely applied and preferred to characterize the winding loss accounting for all these complex effects [10], which can be categorized as three types: 1) the calorimetric (thermal) method [10], [14]–[15]; 2) the electrical impedance analyzer approach [11], [16]–[17]; 3) the direct electrical in-situ measurement [10]. Although the thermal method is relatively reliable, it is difficult to set up and requires a time-consuming procedure to reach the thermal steady state. Additionally, it is challenging to exclude core loss from the total losses to find an accurate winding loss [10], [14]–[15]. Hence this paper will mainly consider the electrical approaches, for which the following challenges should be carefully addressed.

Firstly, when evaluating the winding loss, the magnetic core should be kept attached instead of removed. Otherwise, the effects associated with the electromagnetic fields influenced by the core will not be evaluated [10]–[11]. Measuring the

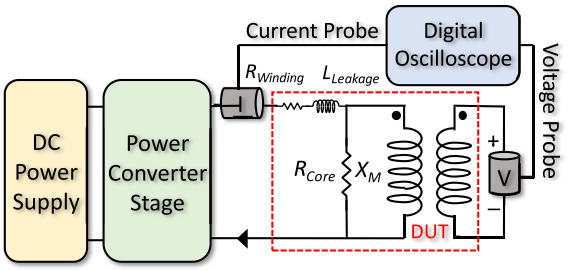

FIGURE 1. Two-winding measurement method.

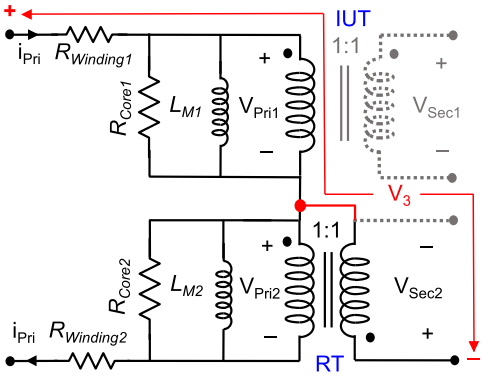

FIGURE 2. The proposed winding loss measurement circuit.

winding loss without the core attached would lose the proximity effect [16] and the effect of core gap fringing flux [12]. But, with the core attached, it will bring challenges of separating the core loss and the winding loss. In short, to accurately characterize the winding loss, the empirical method should be performed with the core equipped while it has the ability to accurately separate the core loss and the winding loss.

Secondly, comparing the impedance analyzer approach with the in-situ measurement, it is reported in the literature that the small-signal measurements cannot completely reflect the property in a large-signal situation for magnetic components [16]. With the presence of large-signal amplitudes or dc-bias, the effective core permeability will vary from the static value [18]–[19] which will influence the magnetic field distribution around the winding and subsequently impact the winding loss as pointed out in [12], [20]. In short, in-situ large-signal measurement should be considered more accurate than small-signal approaches because it reflects the property of the inductor under large-signal or dc-biased excitation that occurs in a real circuit.

Thirdly, for in-situ electrical measurement, the phase discrepancy error is the biggest challenge, which is the difference between the true and measured phase shift between the captured voltage and current signals. On one hand, if the winding loss is obtained indirectly from subtracting the core loss (e.g., measured from the 'two winding method' measurement which is shown in Fig. 1 [1- 4]) from the total loss, both the core loss and total loss are sensitive to the phase discrepancy,

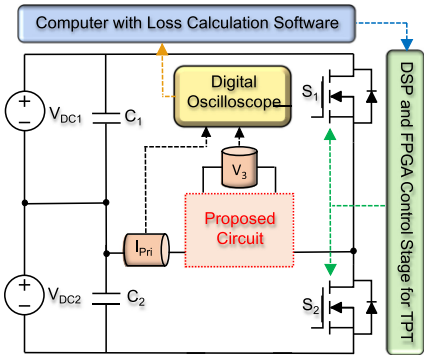

FIGURE 3. Simplified schematic of the power stage.

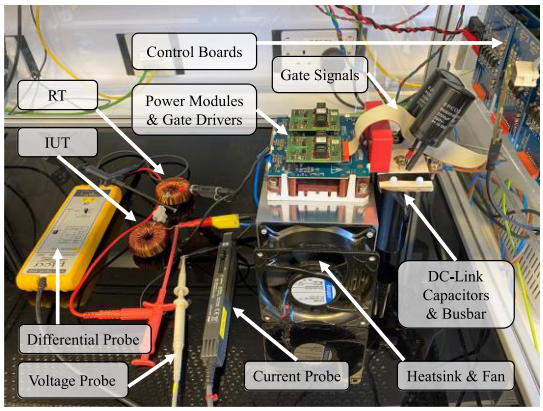

FIGURE 4. The test rig utilized for measuring the proposed winding loss.

on top of each other. In this case, the presence of phase discrepancy error is considerable for the low permeability or gapped cores, which has a high-quality factor (Q) [1], [21]. On the other hand, if the winding loss is measured directly, the phase discrepancy problem will directly impact the winding loss measurement. Hence, the majority of the existing in-situ methods suffer from phase discrepancy [10]–[11]. The phase shift discrepancy can cause a substantial error in measuring the winding loss, especially in cases with higher frequencies [15], [22].

There is a scarcity of existing work regarding empirical winding loss measurements under large-signal excitations. For example, [11], [16], [23] presented a method to obtain the AC resistance of the magnetic component winding utilizing impedance analyzers. These methods are bounded to the limitations of impedance analyzers that evaluates the winding loss under small-signal operation only. Hence, they cannot fully reflect the winding loss properties in large-signal operations. [10] proposed a winding loss measurement method to find the R_{AC} of a planar transformer in a high-frequency SMPS under large-signal excitation, which separates the core loss from the winding loss. However, this method is sensitive to phase discrepancy error.

Another common method to find the winding loss is finite element analysis (FEA). However, FEA simulations have several limitations in finding accurate winding loss, such as the requirement of accurate geometric information of the winding. Therefore, for the inductors with random windings, it is very difficult to exactly replicate their physical structure, which means the FEA simulation cannot accurately reproduce the winding loss in this case. As a result, the complex effects such as proximity, edge, and end effects are not perfectly realized. Additionally, in typical FEA software packages such as Ansys Maxwell [24], the magnetic core permeability is oversimplified as a fixed value at one frequency and magnetic field H, following the magnetic core datasheet that was measured from sinusoidal excitations. This oversimplification limits the FEA methods to find the real winding loss considering the variation of the dynamic core permeability and field interaction between the core and the winding.

Additionally, there are some commercial measurement devices for measuring power inductors losses under real, large-signal conditions, which are used in the laboratories, such as MADMIX [25]. However, they still have some limitations. For instance, the voltage amplitude of the MADMIX is restricted to 0-70 V, and the flux excitation is limited to a triangular shape. Also, these systems are mostly expensive and hard to afford.

Based on the reasons above, this paper proposes an in-situ measurement method, which is mainly a testing circuit, to accurately assess the winding loss under actual waveforms in power converters. The proposed method is insensitive to the phase discrepancy error and can account for all non-ideal high-frequency and large-signal effects. This approach is simple to tune and implement compared to the other reactive voltage cancellation methods [15], [22], [26]–[27]. The winding loss is measured independently from the core loss, which is useful to investigate the winding loss on its own. Although obtaining the overall magnetic component characteristics (winding loss + core loss) is the ultimate goal, measuring each part separately is more helpful to find out which part of the system needs to be redesigned or improved.

In the following, Section II will describe the proposed winding loss measurement method and Section III will present the experimental evaluation, the results analysis and comparison with other existing methods. And finally, Section IV will analyze the proposed method sensitivity regarding the various practical issues.

II. PROPOSED IN-SITU WINDING LOSS MEASUREMENT METHOD

This paper proposes a testing circuit in Fig. 2 to accurately measure the winding loss, which is inspired by the reactive voltage cancellation concept [15], [22], [26]–[27] and the two-winding method for core loss measurement.

To extract the winding loss, a reference transformer (RT) is utilized, which is ideally identical to the inductor under test (IUT) in terms of core and winding specifications. The idea of the proposed approach is to use the RT to cancel out the

reactive voltage as well as the core loss and solely capture the winding loss of IUT. The core loss component of RT is obtained through the secondary voltage on the magnetizing inductance of the RT as shown in Fig. 2, which is reversed to cancel out the core loss component in V_{Pri}. The core loss of IUT does not need to be measured by using the secondary winding, which is greyed out in Fig. 2. When IUT is excited, V_3 is the summation of the IUT primary voltage (V_{Pri}) and the RT secondary winding voltage (V_{Sec2}) as

$$V_3 = \left(Z_1 + R_{Winding1} - Z_2\right) I_{Pri} \tag{2}$$

$$Z_1 = \left(j\omega L_{M1} \parallel R_{Core1}\right), \quad Z_2 = \left(j\omega L_{M2} \parallel R_{Core2}\right) \tag{3}$$

where L_{M1} and L_{M2} are the magnetizing inductances; R_{Core1} and R_{Core2} are the core loss resistances for the IUT and RT, respectively; $R_{Winding1}$ represents the IUT winding resistance. As intended, the IUT and RT are entirely identical to each other (i.e., the same core type and the number of windings). Hence, $L_{M1} = L_{M2}$ and $R_{Core1} = R_{Core2}$, which results in V_3 expressed as

$$V_3 = R_{Winding1} I_{Pri} \tag{4}$$

In reality, these two conditions cannot be met perfectly. Hence a sensitivity analysis is added in Section IV. A to evaluate the potential error when $L_{M1} \neq L_{M2}$ and $R_{Core1} \neq R_{Core2}$. Equation (4) shows that the secondary voltage of the RT cancels the reactive voltage as well as the core loss on the IUT. To obtain V_3, an auxiliary winding is fitted to the RT as shown in Fig. 2. This winding is an open circuit and does not need to carry current. Consequently, V_3 will be considered as the resistive voltage on the winding. By performing (5), the winding loss can be attained as

$$E_{Winding} = \int_0^T I_{Pri}(t) \; . \, V_3(t) \; dt \tag{5}$$

where T is the period of the frequency. In this case, V_3 will be in phase with the I_{Pri}, in contrast to the nearly 90° phase angle between V_{pri} and I_{Pri}. Subsequently, integrating the product of V_3 and I_{Pri} through expression (5) will be significantly less sensitive to the phase shift error [15], [22], [26]–[27]. Therefore, the proposed method can measure the in-situ winding loss for any arbitrary excitation without concerning about the phase discrepancy.

To sum it up, the proposed method is the first and only experimental approach that separates out the complete winding loss with the presence of the core and directly measures it (V_3 and I_{Pri} are basically the voltage and current on the resistive part of the winding). This feature makes it insensitive to phase discrepancy. Additionally, this method can be considered as the first attempt of applying the reactive voltage cancellation concept in measuring winding loss, while this concept was originally brought up for core loss measurement. For multi-winding inductors and transformers, the proposed approach can still be applied in theory and the principle of the approach will stay the same.

TABLE I Components and Instruments in the Test Rig

Power Supplies	Elektro-Automatik TS 8000 T
Voltage Probe	Keysight N2862B (150 MHz)
Differential Probe	Pico TA041 (25MHz)
Current Probe	Keysight N2783B (100 MHz)
Power Module	Semikron SKiM301TMLI12E4B
Gate Driver	Semikron SKYPER 42 J
Digital Oscilloscope	MSO-X 3054A (500 MHz, 4 GSa/s)
DC-Link Capacitance	*C1= C2* =2670 µF
Tested Inductor	92 µH, T184-26,Micrometals©, *N1*:*N2*=24:24

In reality, the IUT and RT have parasitic elements, such as leakage inductance and winding capacitance. Typically, these parasitic elements are insignificant [10]–[11], [15], [22], [26]–[27] and do not undermine the accuracy and immunity against phase discrepancy of the proposed approach. Detailed analysis in this regard will be presented in Section IV.

III. EXPERIMENTAL EVALUATION AND COMPARISON WITH EXISTING APPROACHES

The proposed method is intended to capture the winding loss under the in-situ condition. To reflect the actual operation in a power converter, a typical rectangular voltage and possibly a dc-bias component needs to be applied to the inductor in the testing. To emulate the waveforms seen in a typical power converter, a half-bridge structure [2], [13], [28] depicted in Fig. 3, is utilized to apply rectangular voltage on the testing circuit and conduct bidirectional current, which has the ability to compensate device voltage drops to provide symmetric rectangular voltages.

A triple pulse test (TPT) procedure [2], [28] is implemented to excite the IUT and capture the cycle of interest while it avoids unnecessary continuous operation and the temperature rise. The core idea of the TPT is to run required cycles only (e.g., three pulses) to reach the steady-state, and avoid further useless operations while obtaining the same results as continuous testing. As a result, TPT does not require the full continuous operation capability of the converter and the inductor while it can perform high-power (e.g., hundreds of volts and amps) in-situ testing.

The components and instruments utilized in the test rig are shown and listed in Fig. 4 and Table I, respectively. The proposed method can be adapted in a wide range of cases with various excitation signals, frequency range and inductance range of the IUT. From the excitation circuit point of view, the proposed testing circuit (IUT+RT) can be plugged into any excitation circuit to test the in-situ winding loss. The setup in this work can generate a square-wave voltage ranging between ± 600 V and a dc-bias current ranging from 0 to approximately 200 A. The presented in-situ method can accurately evaluate the large-signal effect when it captures the complete winding loss. Regarding the frequency, as limited by the switching speed of the Silicon IGBTs at the level of microseconds, the frequency range of the producible square wave is up to 150 kHz in the presented setup.

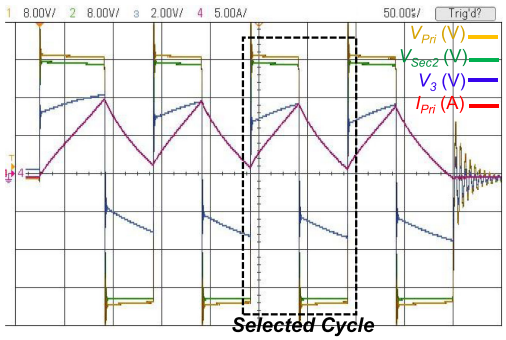

FIGURE 5. Experimental current/voltage waveforms of one TPT test point.

Fig. 5 shows the waveform captured in one test run to measure the winding loss of the inductor presented in Table I by the TPT and proposed circuit. The initial wider pulse is to establish a required dc-bias current (I_0), which is 5 A here. The amplitude of the inductor voltage (V_{Pri}) is fixed to 25 V at 10 kHz. Then, the V_3 is measured, which is the voltage difference between the V_{Pri} and V_{Sec2} as in (4) and depicted in Fig. 5 for this test run. Consequently, the winding loss of the inductor is worked out by equation (5) for the selected cycle, the cycle that the inductor reaches the steady-state where the waveforms are stabilized and captured for calculating the loss as demonstrated in Fig. 5.

To validate the proposed method, two common empirical approaches are considered as the benchmark: (1) the impedance analyzer + FFT analysis (FFT method) (2) the two winding method to measure the total loss deducing the core loss (Indirect method).

For the FFT method, the primary current flowing through the inductor is decomposed into the AC and DC components with FFT in MATLAB across the frequency spectrum for the target cycle. Meanwhile, the AC and DC winding resistances of the inductor are measured by the impedance analyzer across the frequency spectrum. The winding loss can be worked out by expression (1) by summing the winding losses for all frequency components.

The two winding method is commonly used to measure magnetic component losses empirically and is regarded as a universal technique [1]–[4]. Integrating the product of voltage drop across the IUT secondary open-circuit winding (sensing winding) and the current flowing through the primary winding yields the core loss of the inductor as following:

$$E_{Core} = \frac{N_1}{N_2} \int_0^T I_{Pri}(t) \ . V_{Sec}(t) \ dt \tag{6}$$

where N_1 and N_2 are the numbers of the primary and secondary winding turns, respectively. This method has the advantage of being easy to set up for both steady-state or transient measurements and suitable for arbitrary wave excitation. By substituting the V_{Sec} with V_{Pri}, the two-winding method can measure not only the core loss but also the total loss of the IUT [22].

$$E_{Total} = \int_0^T I_{Pri}(t) \ . V_{Pri}(t) \ dt \tag{7}$$

In this case, the difference between E_{Total} and E_{Core} can be used to find the IUT's winding loss [11].

$$E_{Winding} = E_{Total} - E_{Core} \tag{8}$$

Fig. 6 illustrates a comparison of the winding loss results of the tested inductor with three methods. The experiment is performed with three sets of primary voltages, 25, 50, and 75 V, and three frequencies at 10, 50, 100 kHz. In general, the outcome of the proposed method shows a top-level agreement with the other two methods in different conditions, which indicates that the proposed method can exclude the core loss successfully.

In lower frequency, lower dc current, and lower voltage amplitude cases, the other two methods (the FFT + impedance analyzer method and the indirect method) are relatively reliable. In this case, three methods show good consistency, which verifies the accuracy of the proposed approach. For example, when the conditions are $V_{Pri} = 25$ V, 10 kHz, and $I_0 = 0$ A, the differences between the proposed method and the two other methods are only 1% and 2%, respectively. In the higher frequency and amplitude cases, the differences between the three methods are bigger as shown in Fig. 6. For example, when the conditions are V_{Pri}=75 V, 100 kHz, and $I_0 = 20$ A, the differences between the proposed method and the two other methods are increased to 19% and 12%, respectively. It is believed that this mismatch is caused by the limitations of the impedance analyzer approach and the phase discrepancy error in the indirect method. It is also noticeable that the proposed method consistently captures more winding loss than the other two methods in these cases, which is believed to be more comprehensive for the following reasons.

As mentioned, the impedance analyzer approach is based on small-signal measurements, which cannot reflect the whole property of the inductor under large-signal operations (e.g., high amplitudes and dc-bias) [16]. For example, the maximum dc-bias current and voltage that can be generated in the impedance analyzer Wayne Kerr 6500B is about 100 mA_{DC} and 40 V_{DC}. Also, for the generated AC voltage and current, the maximum amplitudes are about 1V_{rms} and 20 mA_{rms}, respectively, which vary with the frequency. Consequently, this limitation of the impedance analyzer prevents it to capture the property of the components entirely under the real large signals. Additionally, [11] points out that impedance analyzers have poor performance for high Q inductors, with the accuracy dropping considerably at higher frequencies. To sum it up, the impedance analyzer has limitations in capturing the winding loss (R_{AC}) in the case with high amplitudes/dc-bias, high frequency as well as high-Q inductors. In contrast, these properties are entirely reflected in the proposed in-situ method with the results shown in Fig. 6.

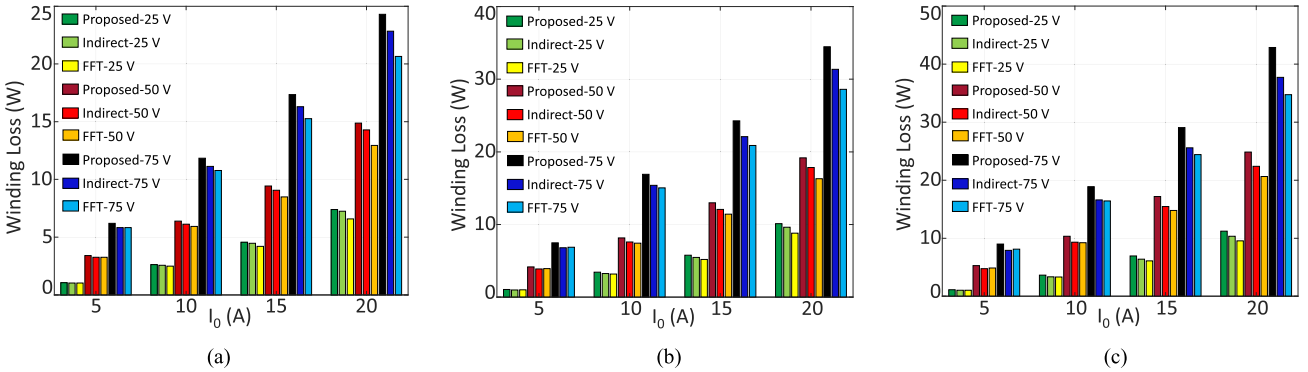

FIGURE 6. Experimental results of the winding loss for the inductor by the proposed method, impedance analyzer + FFT analysis (FFT), and two winding method (Indirect), with the various combination of primary voltage (V_{Pri}) and dc-biased current (I_0) for (a) 10 kHz, (b) 50 kHz, and (c) 100 kHz.

Additionally, the real part of the magnetic component's impedance, R_{M}, obtained from the impedance analyzer includes both the winding loss, R_{W}, and the core loss, R_{C}, components. However, the retrieved R_C is insignificant for the cases where the magnetic component has a low-loss core or the operating frequency is lower than hundreds of kilohertz [16]. Hence it can be considered that $R_{\mathrm{W}} \approx R_{\mathrm{M}}$ in the results of Fig. 6, because a low-loss powdered core is used with the insignificant core loss in the small-signal testing, which leads to little contribution to R_M considering the operating frequencies is below 100 kHz. Therefore, the resistance extracted by the impedance analyser can be considered as reflecting only the winding loss in the illustrated cases. When the core loss becomes significant (e.g., at a high frequency), the measured R_{M} should be considered as $R_{\mathrm{W}} + R_{\mathrm{C}}$.

Secondly, regarding the indirect method, according to previous studies such as [1], [10], [21], the phase discrepancy further deteriorates at higher frequencies and excitation voltages. Therefore, this is the main reason that the indirect method has mismatches at higher inductor voltages and frequencies in Fig. 6. Corresponding to the expression (8), because both the E_{Total} and E_{Core} have their inherent phase shift error, and these errors are added together for calculating the winding loss, this method is more vulnerable to the phase shift error compare to solely measuring the core loss. In contrast, in the proposed approach, the measured pair of voltage and current is in phase by design, which makes it nearly insensitive to the probe phase discrepancy. Hence the proposed approach is superior to the indirect method in this regard. Either the impedance analyzer or the indirect methods cannot evaluate the winding loss in a way that accounts simultaneously for both large-signal effects and insensitivity to the phase shift error.

To further demonstrate the effect of dc-bias, high amplitude, and phase discrepancy against winding loss, Figs. 7, 8, and 9 depict the experimental results of the post-processed equivalent total R_{AC} of the tested inductor. The equivalent total R_{AC} is defined as

$$R_{AC} = \frac{P_{Winding\ (AC)}}{{I_{Pri}}^2{}_{(RMS)}} \tag{9}$$

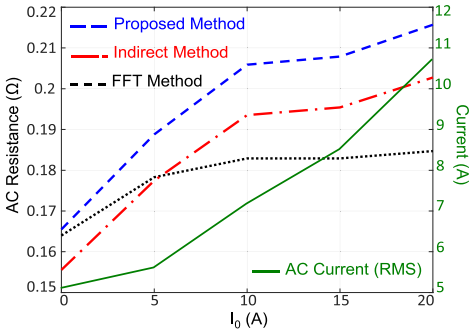

FIGURE 7. Experimental results of the winding's AC resistance for different dc-bias currents at 10 kHz (V_{Pri} = 75 V) and its corresponding AC current (RMS).

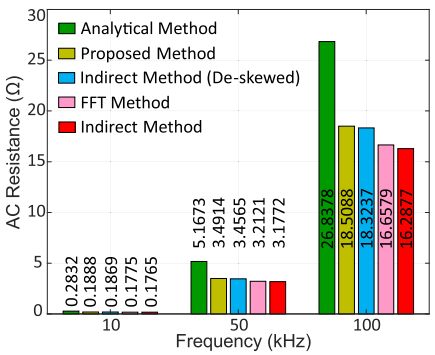

FIGURE 8. Experimental results of the winding's AC resistance by the various approaches when I_0 = 5 A and V_{Pri} = 75 V.

As an approximation, the RMS value of the primary current is retrieved as the peak value divided by $\sqrt{3}$, assuming the current shown in Fig. 5 is triangular. The $P_{Winding(AC)}$ is the total AC winding loss found by the proposed, FFT, and indirect methods, which excluded the DC component $P_{Winding(DC)}$ from the total $P_{Winding}$.

Fig. 7 shows the equivalent total R_{AC} against the dc-bias current I_0, which shows that the R_{AC} witnesses a significant increase with the rising of dc-bias current, e.g., +30% from 0 A to 20 A. This phenomenon is caused by the variation

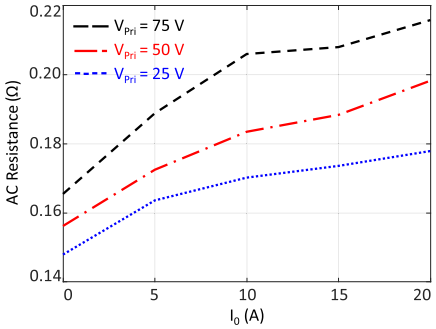

FIGURE 9. Experimental results of the winding's AC resistance by the proposed method at 10 kHz for different inductor voltages.

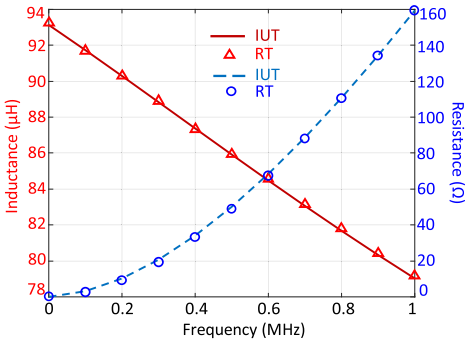

FIGURE 10. The resistances and the magnetizing inductances of the IUT and RT.

of the core permeability at dc-biased condition [4], [18]–[19] and subsequently the distribution of the magnetic fields on the conductors that changes the proximity effect and edge effect, which impacts the winding loss [12], [20]. Additionally, as can be observed, with the increase of the dc-bias current, the AC current component is also increased, which also reflects that the core permeability varied from the static value. This is an important factor that cannot be evaluated in the analytical equations and the impedance analyser + FFT methods. Consequently, the FFT method leads to results close to the proposed method at a low dc-bias, even better than the indirect method for this frequency range, but they show higher differences at a high dc-bias, which can be seen in Fig. 7. The indirect method can properly detect the variations of the winding loss against the increment of dc-bias current. However, the difference between the R_{AC} of the proposed and indirect methods is due to the phase discrepancy error, which is almost constant with the increase of the dc-bias current as it does not affect the phase shift error [11].

Fig. 8 shows different winding loss methods at fixed dc-bias for three various frequencies. Higher frequencies have adverse impacts on both FFT and indirect method as elaborated before due to the impedance analyzer accuracy and phase discrepancy error, respectively. Since the dc-bias current is not high in the results of Fig. 8, the indirect method is more deteriorate compared to the FFT method, and the difference between them is increased by growing the frequency. To further demonstrate the effect of phase shift error on measuring the winding loss, the indirect method is calibrated through a deskew fixture, Keysight U1880A. Fig. 8 clearly demonstrates that by using the deskew tool, the phase discrepancy error is reduced and the results are close to the proposed method that can completely diminish the effect of phase shift error on measuring the winding loss.

To represent the insufficiency of the analytical method, Fig. 8 also depicts the analytical AC resistances for the inductor presented in Table I. The analytical results are acquired from Dowell's 1-D expression for round conductors which is modified in [5], [29], and converted to the square-wave case. Fig. 8 shows that the calculated analytical AC resistances for square excitation are around 45% higher than the results from the proposed method. As previously reported in [30], Dowell's formula can lead to an error as high as 100% in toroidal inductors and overestimate the winding loss significantly. The results illustrated in Fig. 8 suggest that Dowell's equation has a substantial discrepancy compared to the other methods in our tested case with round conductors and random-wound windings, which agrees with [30]–[33].

In addition, as shown in Fig. 9, when the inductor voltage is increased, the R_{AC} found by the proposed method is also increased, which indicates that higher voltage amplitude can also affect the R_{AC}, due to the increment of the non-ideal fringing fields around the core and windings [17].

These factors justify the implementation of the proposed in-situ approach, which reflects these non-linear features and subsequently offer higher accuracy for practical cases.

IV. SENSITIVITY ANALYSIS

A. IMPACT OF RT MISMATCH

As the principle of the proposed approach, it should be highlighted that the RT is intended as a duplicate of the IUT. The proposed method should ideally meet two conditions, $L_{M1} = L_{M2}$ and $R_{Core1} = R_{Core2}$, to measure the error-free winding loss of IUT.

Fig. 10 shows the resistances and the magnetizing inductances of the IUT and RT measured from the impedance analyzer, across the frequency spectrum. Although both the IUT and RT are hand-made, they track each other's property very well across the spectrum, with a mismatch of below 0.5%. IUT and RT share the same core and number of winding turns so that the first condition $L_{M1} = L_{M2}$ is met easily. This feature can be considered as one advantage of the proposed method, i.e., requiring an identical cored component, while the similar existing methods require an air-core RT customized for each testing condition [22], [26]–[27].

Additionally, this feature enables the proposed approach to accurately test the cases with the high value of the magnetizing inductances, which is not feasible for other inductive voltage cancellation methods such as Mu's and Hou's methods for core loss measurement; because the achievable inductance of the air-core transformer is limited by the parasitic elements, which could adversely affect the waveforms and the accuracy

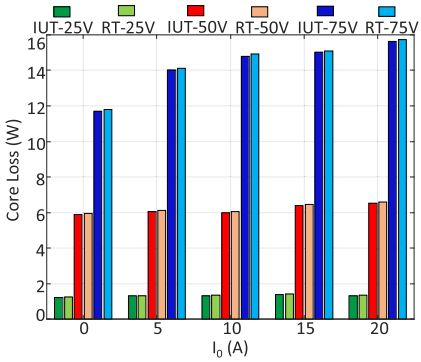

FIGURE 11. **The core losses of IUT and RT at 100 kHz for different operations.**

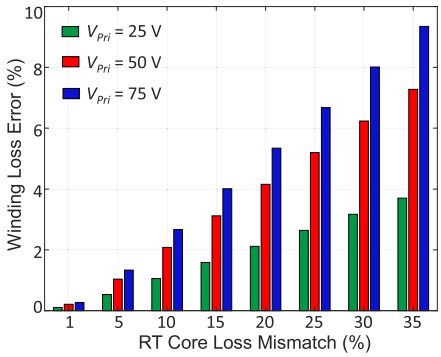

FIGURE 12. **Winding loss measurement error when the RT core loss is not completely matched in comparison with the IUT core loss ($I_0 = 20$ A, $f =$ 100 kHz).**

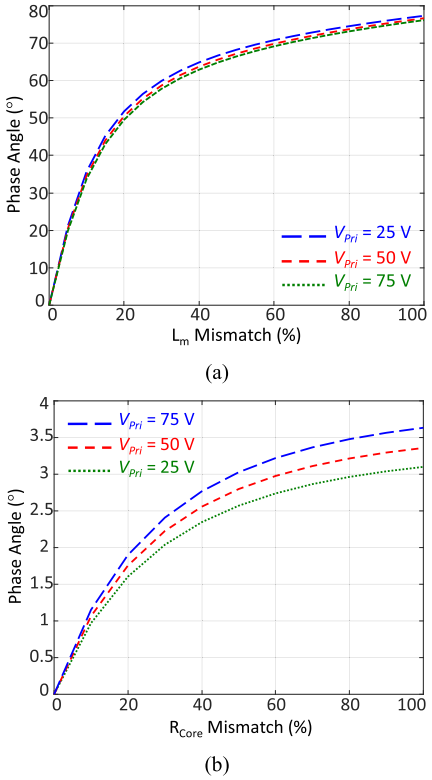

FIGURE 13. **The variation of the phase angle between the V_3 and the I_{Pri}, at $I_0 = 5$ A and $f = 50$ kHz for (a) the mismatches between the magnetizing inductances of the RT and IUT, and (b) the mismatches between the core loss resistances of the RT and IUT.**

of the system especially at higher frequencies [22], [26]–[27], [34]–[36].

Fig. 11 presents the core losses of the IUT and RT, evaluated in TPT for various test operations by two winding method with auxiliary flux sensing windings. The core losses of the two devices are consistent, with a mismatch of below 1%, which is intended to cancel out the core loss and subsequently measure the winding loss of the IUT through (5). Hence, this tested case satisfies the two conditions required to accurately determine a winding loss.

In reality, a mismatch between RT and IUT can occur, e.g., due to batch-to-batch variation of the cores, while ideally, they should be identical. Therefore, the sensitivity between the measured winding loss and the mismatch of the core loss of two magnetic devices is evaluated and presented in Fig. 12. By varying the mismatch of the RT core loss, the resulted winding loss and the error are worked out in comparison to the ideal case. As can be concluded from the results, even when the RT has one-third of the core loss discrepancy (35%), the measured winding loss error is still lower than 10%. Considering that a large number of standardized inductors are available today, a reference inductor/transformer with nearly identical properties should be easy to find, as long as the core shape, core material and winding arrangements are intended to stay the same.

Figs. 13(a) and (b) display the variation of the phase angle between the V_3 and the I_{Pri}, when the L_{M2} and R_{Core2} of the RT have mismatches from L_{M1} and R_{Core1} of the IUT, respectively. When both the L_{M2} and R_{Core2} of the RT completely have the same values of the IUT properties as L_{M1} and R_{Core1}, the phase angles between the V_3 and the I_{Pri}, are totally zero. Hence, V_3 is considered as the pure resistive voltage on the winding and in phase with the I_{Pri}. However, Fig 13(a) demonstrates that when the magnetizing inductance of the RT has mismatches from the L_{M1}, the phase angle is rapidly changed and the inductive voltage cancellation method cannot entirely neutralize the reactive voltage. On one hand, since the proposed method using the same core type and the number of windings of the IUT for the RT, it is relatively easy to fulfil a zero phase angle, and easy to match an inductance of 10 $\sim$ 1000 μH that is typical in power converters with a switching frequency of less than a few hundreds of kilohertz [37]. On the other hand, the other inductive reactive voltage cancellation methods for core loss measurement cannot match the IUT magnetizing inductance value as accurate as the proposed method, because they utilize air-cored inductors with a large number of windings to reach the matching inductance, which can lead to significant parasitic components and subsequently significant error of measurement [22], [26]–[27], [34]–[36].

Additionally, Fig. 13(b) shows the impact of the mismatch of the core loss resistance R_c. As can be seen, the mismatch

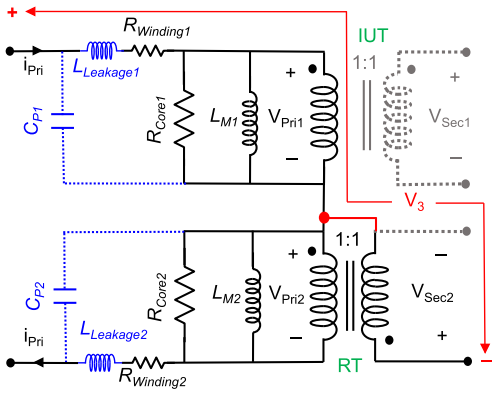

FIGURE 14. Equivalent circuit of the proposed method with parasitic elements associated with the IUT and RT.

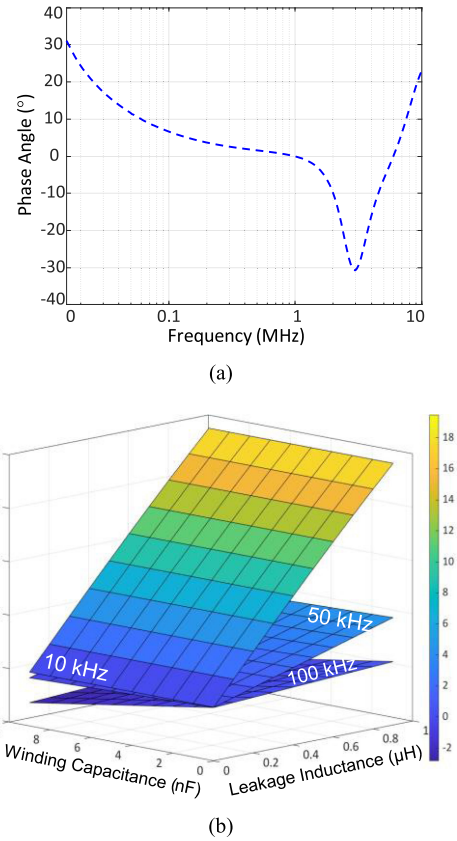

FIGURE 15. (a) The phase of the impedance considering the parasitic capacitance, leakage inductance, and winding resistance of the IUT. (b) The impedance phase angle of the IUT for three different frequencies of the square excitation voltage used in the experiment in the variation of the leakage inductance and winding capacitance ($I_0 = 0$ A and $V_{Pri} = 25$ V).

of core loss does not change the phase angle as significant as the magnetizing inductance variations. In short, considering the mismatch between the RT and IUT, the magnetizing inductance is more influential and the core loss is less of an issue, while both of them can be relatively easily minimized in the proposed approach as a result of requiring the same device.

B. IMPACT OF PARASITIC ELEMENTS

In practice, magnetic components have parasitic elements, such as leakage inductance and distributed capacitance, that may impact the proposed approach's sensitivity to probe phase discrepancy. These two factors can be modelled as in the equivalent circuit shown in Fig. 14.

The first concerning parasitic element is the leakage inductance, which is caused by the leakage flux. Any magnetic flux not linking the primary winding to the secondary winding acts as a leakage inductive impedance in series with the primary magnetizing inductance [5]. The leakage inductance of inductors (e.g., $L_{Leakage1}$) is generally small, e.g., $< 0.5\%$ of the magnetic inductance [5].

The second concerning parasitic element is the winding capacitance which can be modelled as a parallel branch [5], [16] as shown in Fig. 14. The C_{P1} and C_{P2} are the lumped parasitic capacitances which include the turn-to-turn and turn-to-core distributed capacitance [5], [15], [22] for the IUT and RT. This winding capacitance in most cases is insignificant in general [5], [10], [11], [15], [22], [26]–[27]. The error of the parasitic capacitance on the reactive voltage cancellation method for the core loss measurement is assessed to be lower than 1% in previous works [15] and [22].

Considering Both Parasitic Elements and (2-4), the Leakage Inductance and Parasitic Capacitance Can Be Concerned in the Measured V_3 as

$$V_3 = \left(\left(j\omega L_{Leakage1} + R_{Winding1} \right) \parallel \frac{1}{j\omega C_{P1}} \right) I_{Pri} \qquad (10)$$

In this case, equation (5) still yields the real winding loss over an integer number of signal cycles, while the presence of the leakage inductance and winding capacitance together can lead to a phase shift of the measured signal pair V_3 and i_{pri} by introducing the reactive components, especially at high frequencies, which may impact the proposed approach's immunity against probe phase discrepancy.

To investigate this issue, the leakage inductance of the IUT/RT can be measured by an impedance analyzer or LCR meter with a short circuit applied across the secondary terminals of the magnetic component, which equivalently shorted out the magnetizing inductance. In this case, the measured inductance of the primary winding is the leakage inductance [38]. The $L_{Leakage1}$ of the tested IUT is measured at around $0.47 \sim 0.49$ μH, which is about 0.5% of the magnetizing inductance of the IUT. The winding capacitance of the IUT/RT can also be accurately measured by an impedance analyzer or LCR meter at a frequency above the self-resonant frequency [5], [16], which is measured at 15 pF at 3.5 MHz for the studied IUT.

Fig. 15(a) plots the phase angle between the signal pair V_3 and i_{pri} in (10) considering the measured $L_{Leakage1}$, C_{P1} and $R_{Winding1}$. Note as the frequency increases, while the impedance of the leakage inductance ωL rises linearly, the real part in (10), the AC winding resistance, can also rapidly

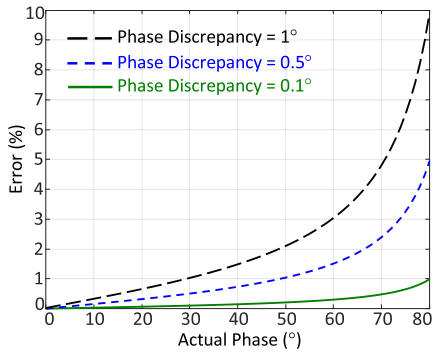

FIGURE 16. Relationship between the error of measured real loss and the assumed probe phase discrepancy.

increase due to the skin effect and proximity effect. Therefore, factoring in both the reactive and the real parts in (10), Fig. 15(a) shows a complex change of phase angle against frequency. Nevertheless, it can be seen that the phase angle between V_3 and i_{pri} is always below $\pm 30°$ from a low frequency to up to 10 MHz in this case. Also, between 50 kHz and 2 MHz, it is lower than $\pm 10°$, while the self-resonance frequency of the DUT is measured at around 3 MHz.

Fig. 15(b) shows the impedance phase angle of the IUT for three different frequencies in the variation of the leakage inductance and winding capacitance values. With the winding resistance measured from the proposed method, according to the (10), the phase angle between the signal pair V_3 and i_{pri} is always lower than $\pm 20°$ for three frequencies tested in the experiment, even if we assume an exaggerated 1 μH leakage inductance and 10 nF parasitic capacitance. Additionally, as illustrated in Fig. 15(b), since the winding capacitance typically has a small value, its impact on the phase angle is much lower than the leakage inductance. These observations from Fig. 15 should also apply to typical cored inductors regardless of the core material, because the common engineering practice always intends to minimize the leakage inductance and the parasitic capacitance.

In summary, in the proposed method, the typical phase shift between the signal pair V_3 and i_{pri} in (10) should be less than $\pm 30°$ when the frequency is $<$ 10 MHz, considering the nonideal parasitic elements and the growth of AC winding resistance at a high frequency. Hence, a phase discrepancy of the probes does not lead to a significant error on the measured winding loss. Also, taking the leakage inductance into account means this method can account for the losses both in the winding and those linked to the leakage inductance.

Fig. 16 shows the relationship between the error of measured real loss and the assumed probe phase discrepancy [1]. When the measured phase angle is lower than 30°, a 1° phase discrepancy of the probes leads to an error of only $<1\%$. With (5) yielding the real winding loss only over the integer number of cycles regardless of the reactive elements, the proposed approach can still be considered to have immunity against probe phase discrepancy. Hence, from the frequency point of view, the proposed approach can be accurately adopted to evaluate the winding loss in a frequency range from 0 Hz to approximately 10 MHz. Fundamentally, this approach is designed to exclude the core loss element and capture the real winding loss only, while the parasitic reactive components are relatively insignificant in this process. Additionally, regardless of the immunity of the proposed method, the measuring probes should always be calibrated to an extent to diminish the phase discrepancy error, e.g., through the deskew function of the oscilloscope and a deskew tool, which is particularly recommended for the inductors with high leakage inductance or parasitic capacitance.

V. CONCLUSION

This paper proposes a new in-situ testing approach to accurately measure the winding loss of a given magnetic component with the presence of the magnetic core. The proposed method completely captures the whole winding loss, including the impacts from the non-ideal field distributions on the magnetic components and non-linear large-signal effects. Compared to other electrical measurement methods, the main superiority of the presented method is the immunity to phase discrepancy and the exclusion of core loss to capture the winding loss only. Also, due to the easy attainability of the required reference transformer, the proposed method is simple to implement compared with the other reactive voltage cancellation methods. The proposed method can enable quick and accurate winding loss characterization to form a datasheet of a standardized inductor to inform the power converter design for practical purposes, which will be covered in future work.

REFERENCES

[1] V. J. Thottuvelil, T. G. Wilson, and H. A. Owen, "High-frequency measurement techniques for magnetic cores," *IEEE Trans. Power Electron.*, vol. 5, no. 1, pp. 41–53, Jan. 1990.

[2] J. Wang, K. J. Dagan, X. Yuan, W. Wang, and P. H. Mellor, "A practical approach for core loss estimation of a high-current gapped inductor in pwm converters with a user-friendly loss map," *IEEE Trans. Power Electron.*, vol. 34, no. 6, pp. 5697–5710, Jun. 2019.

[3] T. Shimizu and S. Iyasu, "A practical iron loss calculation for AC filter inductors used in PWM inverters," *IEEE Trans. Ind. Electron.*, vol. 56, no. 7, pp. 2600–2609, Aug. 2009.

[4] J. Muhlethaler, J. Biela, J. W. Kolar, and A. Ecklebe, "Core losses under the DC bias condition based on Steinmetz parameters," *IEEE Trans. Power Electron.*, vol. 27, no. 2, pp. 953–963, Feb. 2012.

[5] K. K. Marian, *High-Frequency Magnetic Components*, 2nd ed. Chichester, U.K.: Wiley, 2014.

[6] P. L. Dowell, "Effects of eddy currents in transformer windings," *Proc. Inst. Elect. Engineers*, vol. 113, no. 8, pp. 1387–1394, Aug. 1966.

[7] J. A. Ferreira, "Improved analytical modeling of conductive losses in magnetic components," *IEEE Trans. Power Electron.*, vol. 9, no. 1, pp. 127–131, Jan. 1994.

[8] B. Chen and L. Li, "Semi-empirical model for precise analysis of copper losses in high-frequency transformers," *IEEE Access*, vol. 6, pp. 3655–3667, 2018.

[9] F. Robert, P. Mathys, and J. -. Schauwers, "A closed-form formula for 2-D ohmic losses calculation in SMPS transformer foils," *IEEE Trans. Power Electron.*, vol. 16, no. 3, pp. 437–444, May 2001.

[10] Y. Han, W. Eberle, and Y. Liu, "A practical copper loss measurement method for the planar transformer in high-frequency switching converters," *IEEE Trans. Ind. Electron.*, vol. 54, no. 4, pp. 2276–2287, Aug. 2007.

[11] F. N. Javidi and M. Nymand, "A new method for measuring winding ac resistance of high-efficiency power inductors," *IEEE Trans. Power Electron.*, vol. 33, no. 12, pp. 10736–10747, Dec. 2018.
[12] F. A. Holguín, R. Asensi, R. Prieto, and J. A. Cobos, "Simple analytical approach for the calculation of winding resistance in gapped magnetic components," in *Proc. IEEE Appl. Power Electron. Conf. Expo.*, 2014, pp. 2609–2614.
[13] J. Wang, N. Rasekh, X. Yuan, and K. J. Dagan, "An analytical method for fast calculation of inductor operating space for high-frequency core loss estimation in two-level and three-level PWM converters," *IEEE Trans. Ind. Appl.*, vol. 57, no. 1, pp. 650–663, Jan./Feb. 2021.
[14] C. Xiao, G. Chen, and W. G. H. Odendaal, "Overview of power loss measurement techniques in power electronics systems," *IEEE Trans. Ind. Appl.*, vol. 43, no. 3, pp. 657–664, May/Jun. 2007.
[15] M. Mu, Q. Li, D. J. Gilham, F. C. Lee, and K. D. T. Ngo, "New core loss measurement method for high-frequency magnetic materials," *IEEE Trans. Power Electron.*, vol. 29, no. 8, pp. 4374–4381, Aug. 2014.
[16] B. X. Foo, A. L. F. Stein, and C. R. Sullivan, "A step-by-step guide to extracting winding resistance from an impedance measurement," in *Proc. IEEE Appl. Power Electron. Conf. Expo.*, 2017, pp. 861–867.
[17] S. Prabhakaran and C. R. Sullivan, "Impedance-analyzer measurements of high-frequency power passives: Techniques for high power and low impedance," in *Proc. IEEE Conf. IAS Annu. Meeting*, 2002, pp. 1360–1367.
[18] Y. Miwa and T. Shimizu, "Loss comparison of core materials used for the inductor of a buck-chopper circuit," in *Proc. IEEE Energy Convers. Congr. Expo.*, 2015, pp. 5279–5286.
[19] K. Emori, T. Shimizu, and Y. Bizen, "Discussion on design optimization of inductor loss focused on copper loss and iron loss," in *Proc. 1st Int. Future Energy Electron. Conf.*, Tainan, Taiwan, 2013, pp. 241–245.
[20] B. A. Reese and C. R. Sullivan, "The effect of permeability on magnetic core performance factors," in *Proc. IEEE Workshop Control Model. Power Electron.*, 2017.
[21] J. Moon, "In-situ direct magnetic loss measurement in a DC-DC converter," in *Proc. IEEE Energy Convers. Congr. Expo.*, Baltimore, MD, USA, 2019, pp. 1261–1268.
[22] D. Hou, M. Mu, F. C. Lee, and Q. Li, "New high-frequency core loss measurement method with partial cancellation concept," *IEEE Trans. Power Electron.*, vol. 32, no. 4, pp. 2987–2994, Apr. 2017.
[23] K. Niyomsatian, J. J. C. Gyselinck, and R. V. Sabariego, "Experimental extraction of winding resistance in litz-wire transformers—Influence of winding mutual resistance," *IEEE Trans. Power Electron.*, vol. 34, no. 7, pp. 6736–6746, Jul. 2019.
[24] ANSYS Maxwell, Oct. 2021. [Online]. Available: https://www.ansys.com/products/electronics/ansys-maxwell
[25] MADMIX, Power Inductor Measurement, Accessed: Oct. 2021. [Online]. Available: http://www.mindcet.com/measurement-systems/madmix
[26] M. Mu and F. C. Lee, "A new high frequency inductor loss measurement method," in *Proc. IEEE Energy Convers. Congr. Expo.*, Phoenix, AZ, Sep. 2011, pp. 1801–1806.
[27] M. Mu, F. C. Lee, Q. Li, D. Gilham, and K. D. T. Ngo, "A high frequency core loss measurement method for arbitrary excitations," *Proc. 26h Annu. IEEE Appl. Power Electron. Conf. Expo.*, Fort Worth, TX, 2011, pp. 157–162.
[28] J. Wang, X. Yuan, and N. Rasekh, "Triple pulse test (TPT) for characterizing power loss in magnetic components in analogous to double pulse test (DPT) for power electronics devices," in *Proc. Annu. Conf. IEEE Ind. Electron. Soc.*, 2020, pp. 4717–4724.
[29] R. P. Wojda and M. K. Kazimierczuk, "Analytical optimization of solid–round-wire windings," *IEEE Trans. Ind. Electron.*, vol. 60, no. 3, pp. 1033–1041, Mar. 2013.
[30] D. Elizondo, E. L. Barrios, P. Sanchis, and A. Ursua, "Analytical modeling of high-frequency winding loss in round-wire toroidal inductors," in *Proc. IEEE 21st Workshop Control Model. Power Electron.*, 2020, pp. 1–6.
[31] K. V. Iyer, W. P. Robbins, K. Basu, and N. Mohan, "Transformer winding losses with round conductors for duty-cycle regulated square waves," in *Proc. Int. Power Electron. Conf.*, Hiroshima, Japan, 2014, pp. 3061–3066.
[32] Xi Nan and C. R. Sullivan, "An improved calculation of proximity-effect loss in high-frequency windings of round conductors," in *Proc. IEEE 34th Annu. Conf. Power Electron. Specialist*, Acapulco, Mexico, 2003, pp. 853–860.
[33] C. R. Sullivan, "Computationally efficient winding loss calculation with multiple windings, arbitrary waveforms, and two-dimensional or three-dimensional field geometry," *IEEE Trans. Power Electron.*, vol. 16, no. 1, pp. 142–150, Jan. 2001.
[34] F. Zhu, Q. Li, and F. C. Lee, "Improved partial cancellation method for high frequency core loss measurement," in *Proc. IEEE Appl. Power Electron. Conf. Expo.*, Anaheim, CA, USA, 2019, pp. 1430–1435.
[35] Z. Ma, J. Yao, Y. Li, and S. Wang, "Comparative analysis of magnetic core loss measurement methods with arbitrary excitations," in *Proc. IEEE Energy Convers. Congr. Expo.*, Baltimore, MD, USA, 2019, pp. 4125–4130.
[36] N. Rasekh, J. Wang, and X. Yuan, "A new method for offline compensation of phase discrepancy in measuring the core loss with rectangular voltage," *IEEE Open J. Ind. Electron. Soc.*, vol. 2, pp. 302–314, Jan. 2021.
[37] B. Zhao, Q. Song, W. Liu, and Y. Sun, "Overview of dual-active-bridge isolated bidirectional dc-dc converter for high-frequency-link power-conversion system," *IEEE Trans. Power Electron.*, vol. 29, no. 8, pp. 4091–4106, Aug. 2014.
[38] Voltech Instruments, "Measuring leakage inductance," 2001. [Online]. Available: http://www.voltech.com/Articles/104-105/1_What_is_Leakage_Inductance

NAVID RASEKH (Student Member, IEEE) received the B.Sc. degree from the Kermanshah University of Technology, Kermanshah, Iran, in 2015 and the M.Sc. degree from the Amirkabir University of Technology, Tehran, Iran, in 2018, both in electrical engineering. He is currently working toward the Ph.D. degree with the Electrical Energy Management Group, University of Bristol, Bristol, U.K. His main research interests include design and control of the power electronic converters, power loss measurement of magnetic components, wireless power transfer, and finite element analysis.

JUN WANG (Member, IEEE) received the B.S. degree in electrical engineering from Sichuan University, Chengdu, China, the M.Sc. degree in electrical engineering from the University of Nottingham, U.K., in 2014, and the Ph.D. degree in power electronics from the University of Bristol, U.K., in 2019. He is currently a Senior Research Associate with the Electrical Energy Management Group, the University of Bristol. His research interests include PWM power converters, multilevel DC/AC converter topologies, power loss modelling of power devices and magnetic components, design optimization and application of wide-bandgap power devices.

XIBO YUAN (Senior Member, IEEE) received the B.S. degree from the China University of Mining and Technology, Xuzhou, China, and the Ph.D. degree from Tsinghua University, Beijing, China, in 2005 and 2010, respectively, both in electrical engineering. Since 2017, he has been a Professor with the Electrical Energy Management Group, Department of Electrical and Electronic Engineering, University of Bristol, Bristol, U.K. He also holds the Royal Academy of Engineering/Safran Chair in Advanced Aircraft Power Generation Systems. He is the Director of the U.K. National Centre for Power Electronics and an Executive Committee Member of the IET Power Electronics, Machines and Drives network. His research interests include power electronics and motor drives, wind power generation, multilevel converters, application of wide-bandgap devices, electric vehicles and more electric aircraft technologies. He is an Associate Editor for IEEE TRANSACTIONS ON INDUSTRY APPLICATIONS and IEEE JOURNAL OF EMERGING AND SELECTED TOPICS IN POWER ELECTRONICS. He is a Fellow of IET and was the recipient of The Isao Takahashi Power Electronics Award in 2018.